

ARTICLE

Electronic Supplementary Information

I. Synthesis and structural properties



Fig. 1s (a) Representative images of the CuInS₂ quantum dots, used as the core seeds in synthesis of the CuInS₂/ZnS core-shell heterostructures. Evolution of the absorption edge due to spatial confinement of excitons is well seen in the image. Difference in the energy of the first excitonic transition between the largest and the smallest quantum dots was 0.71 eV. The highest energy of 2.55 eV was found for the smallest (yellow sample at the left side) *ca.* 1.6 nm CuInS₂ QDs. Exciton energy for the largest synthesized CuInS₂ QDs was found to be 1.84 eV (*ca.* 3.0 nm). (b) Representative image of paired samples of the CuInS₂ cores (on the right of each pair) and CuInS₂/ZnS (on the left of each pair) core-shell quantum heterostructures. Characteristic blue-shift of the absorption edge can be observed upon the ZnS formation on the CuInS₂ cores.

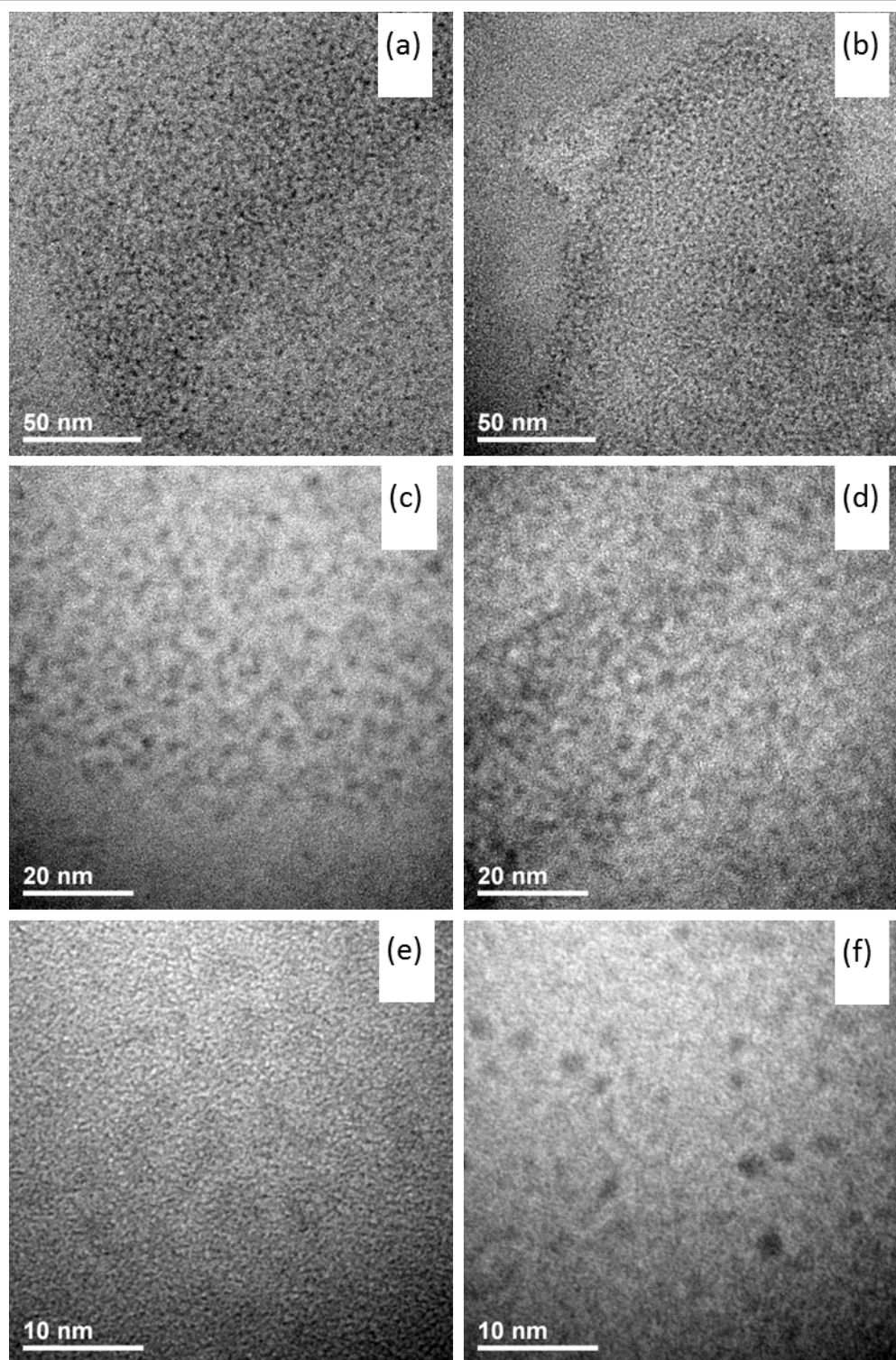


Fig. 2s TEM images of representative *ca.* 3.0 nm CuInS₂ core QDs at magnification (a) x57 000, (c) x135 000, and (e) x300 000. The same sample of CuInS₂ QDs after the ZnS shell formation at corresponding magnification (b) x57 000, (d) x135 000 and (f) x300 000 was also shown. The microstructure of samples was examined with a Philips CM20 SuperTwin transmission electron microscope, which provides a resolution of 0.25 nm at 200 kV.

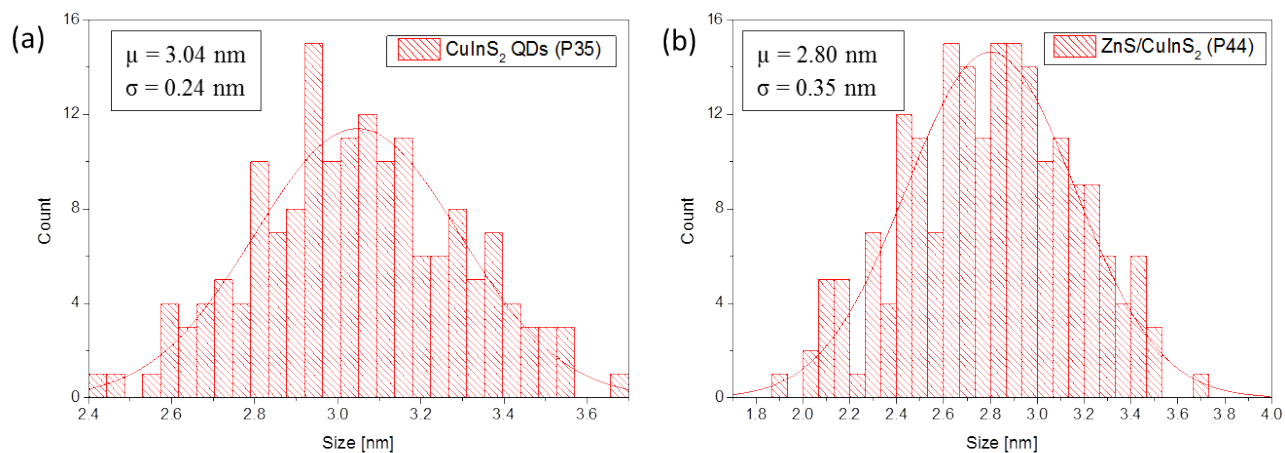


Fig. 3s Histograms of the QDs sizes calculated according to the TEM images taken for (a) *ca.* 3.0 nm CuInS₂ QDs and (b) their corresponding CuInS₂/ZnS quantum heterostructures. Due to the fact that growth of the quantum dots is a stochastic process, normal distribution was assumed in the calculations. According to the normal distribution, mean size of the core CuInS₂ QDs was calculated as *ca.* 3.0 nm with standard deviation $\sigma=0.24$ nm. The mean size of the corresponding core-shell QDs (b) was estimated as $\mu=2.8$ nm with standard deviation of $\sigma=0.35$ nm.

II. Optical properties

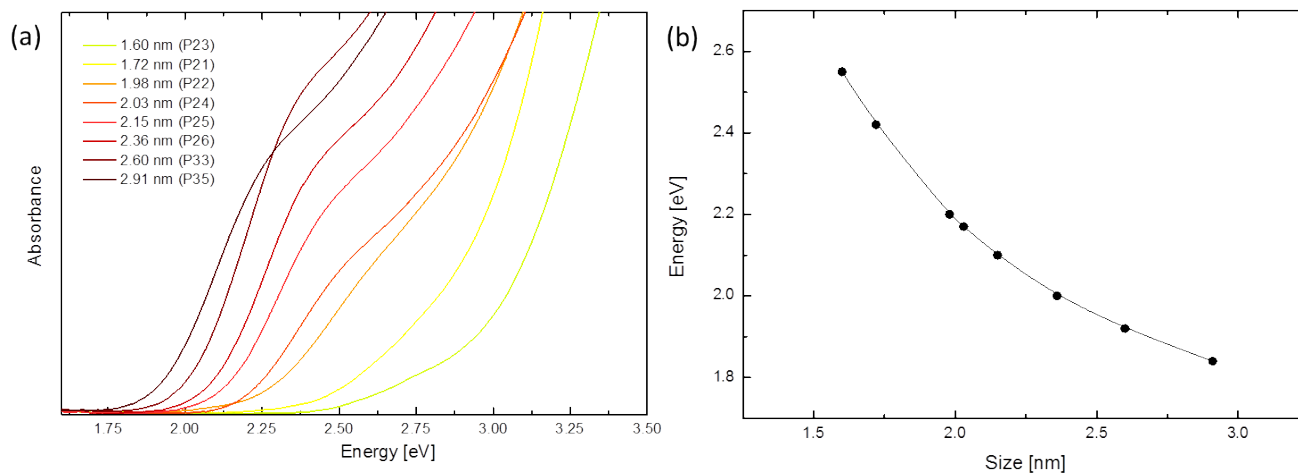


Fig. 4s (a) Size dependent absorption edge shift observed for the CuInS₂ QDs and (b) optical band gap energy replotted as a function of the CuInS₂ QDs

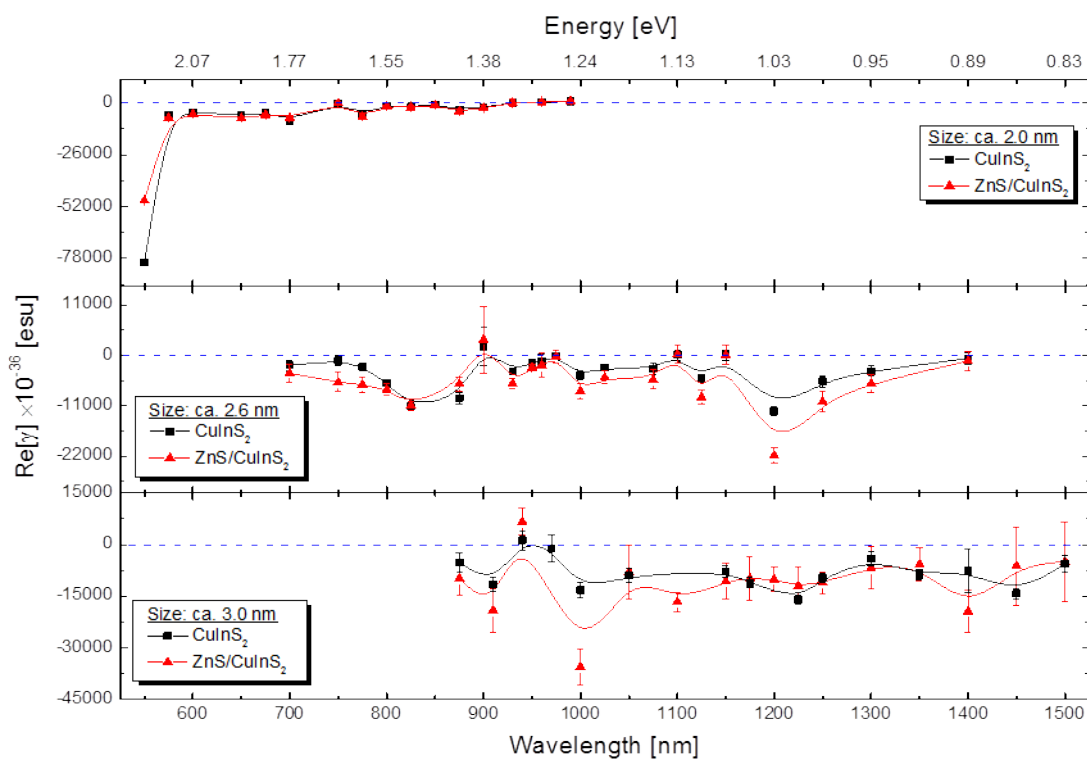


Fig. 5s Dispersion of the real part of the complex hyperpolarizability γ measured for the *ca.* 2.0 nm, 2.6 nm and 3.0 nm CuInS₂ QDs as well as their corresponding CuInS₂/ZnS core-shell quantum heterostructures. Refractive part of γ measured for the core CuInS₂ QDs is plotted in black while results for the CuInS₂/ZnS QDs are plotted in red colour.

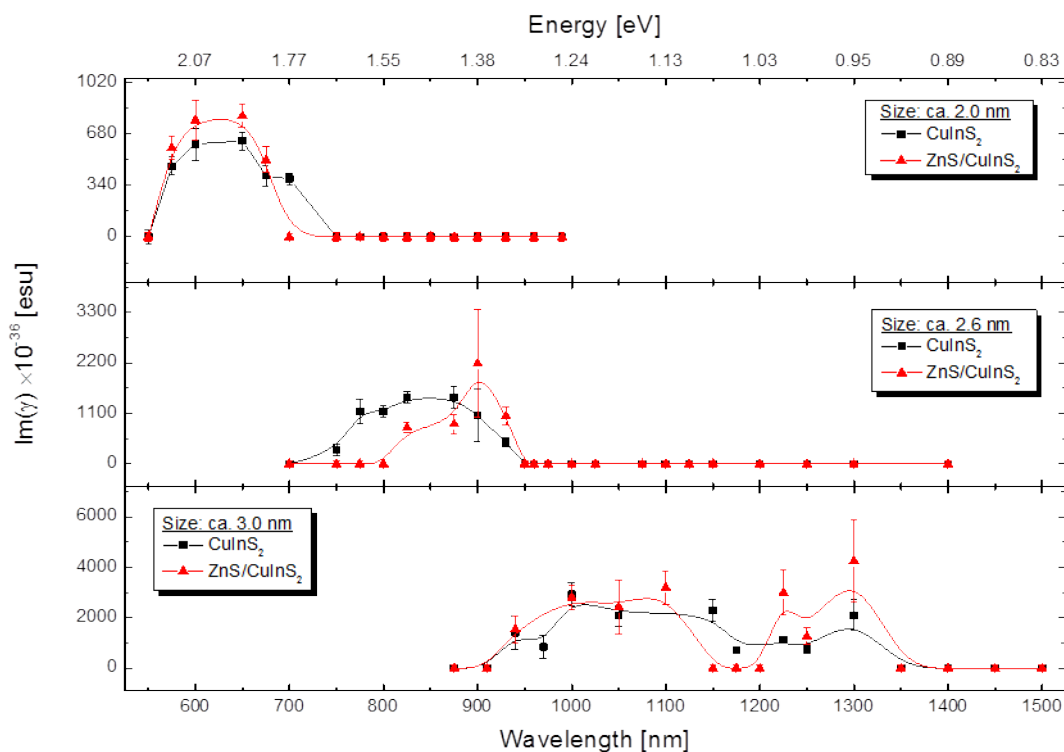


Fig. 6s Dispersion of the imaginary part of the complex hyperpolarizability γ measured for the *ca.* 2.0 nm, 2.6 nm and 3.0 nm CuInS₂ QDs as well as their corresponding CuInS₂/ZnS core-shell quantum heterostructures. Absorptive part of γ measured for the core CuInS₂ QDs is plotted in black while results for the CuInS₂/ZnS QDs are plotted in red colour.

III. Time-resolved spectroscopy

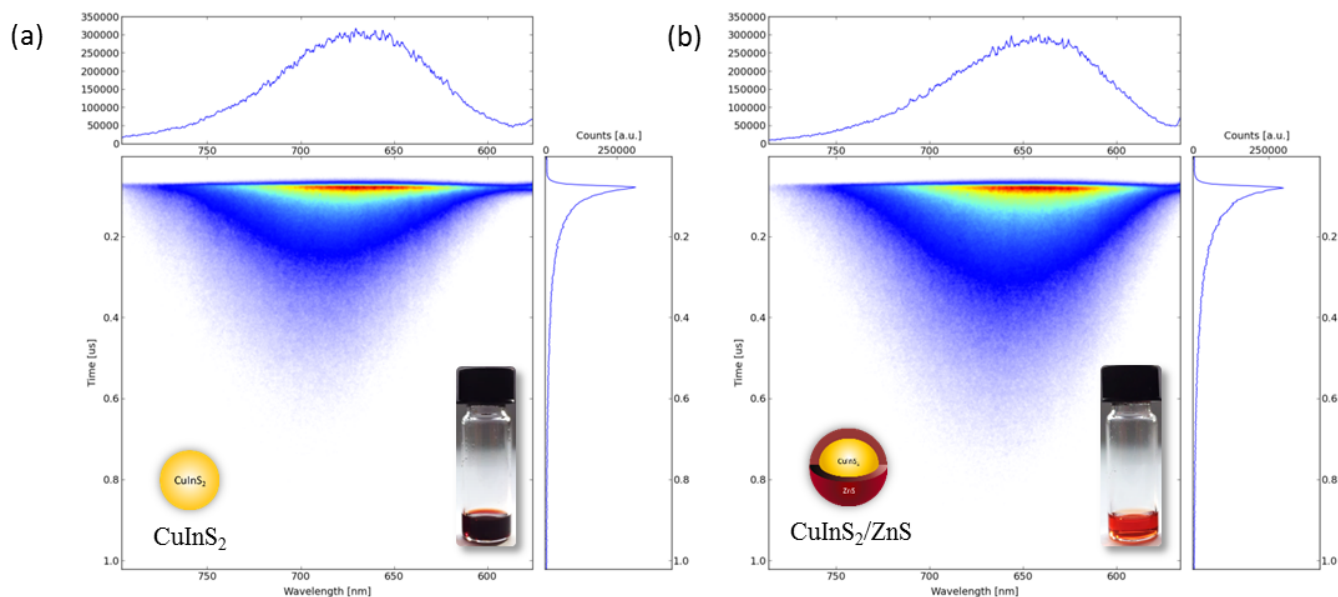


Fig. 7s Time-resolved photoluminescence spectra (TRPL) of single-photon excited ($\lambda_{\text{ex}} = 550$ nm) *ca.* 3.0 nm in size (a) core CuInS₂ QDs and (b) their corresponding CuInS₂/ZnS core-shell quantum dots. Elongation of the fluorescence lifetime as well as slight blue-shift of the emission band after the ZnS shell formation is well seen. Several other features of the TRPL spectra should also be noticed. At first, temporal evolution of the emission band toward lower energies is observed in all the samples (see also Fig 8s). Non-exponential character of the decay curves was observed in all CuInS₂ QDs as well as their corresponding CuInS₂/ZnS heterostructures, indicating that competitive emission from different states characterized by different decay rates is observed in the TRPL spectra.

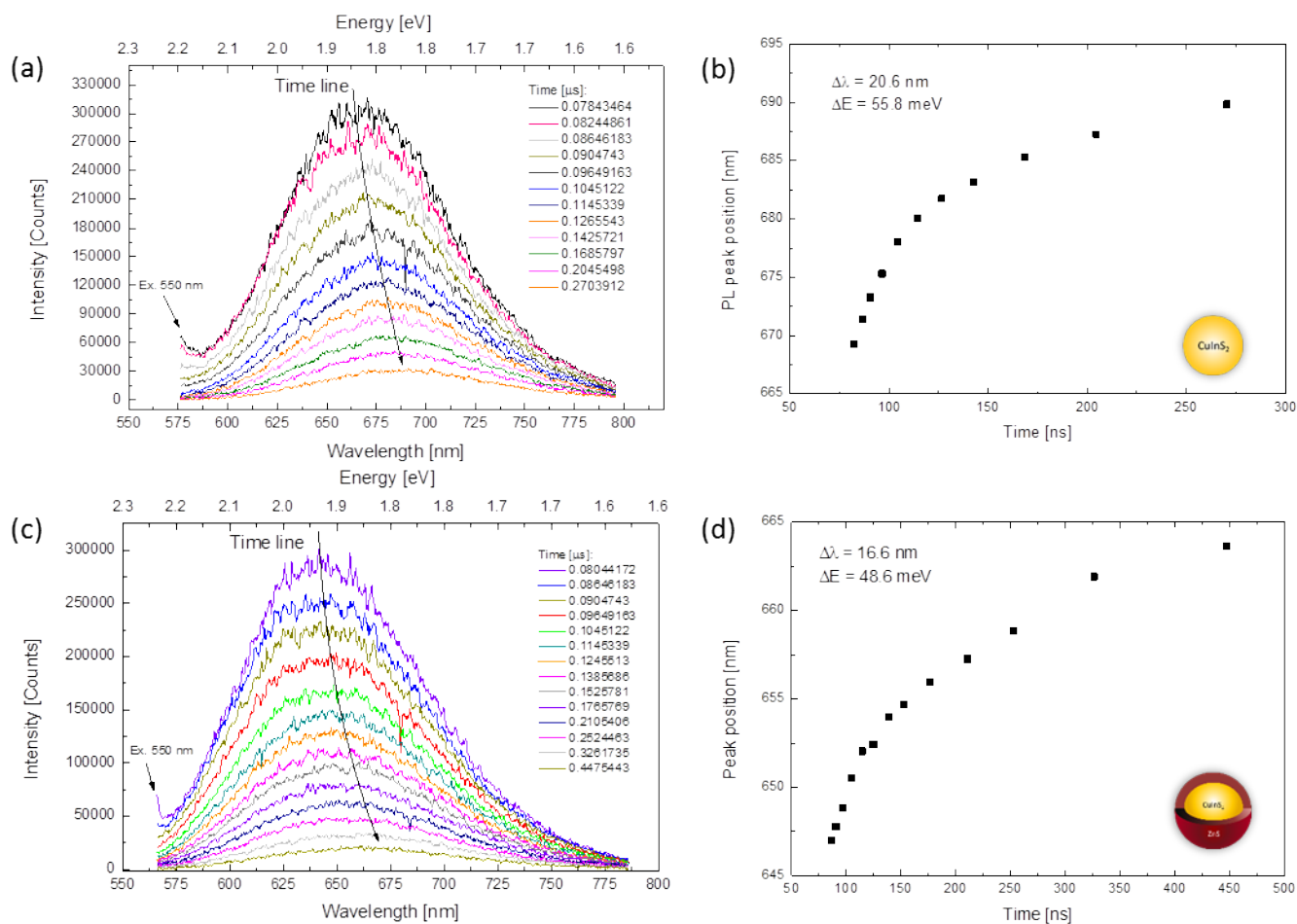


Fig. 8s Time-resolved photoluminescent spectra measured for the *ca.* 3.0 nm CuInS_2 QDs and (c) their corresponding $\text{CuInS}_2/\text{ZnS}$ quantum heterostructures. Temporal evolution of the emission band for the (b) CuInS_2 and (d) $\text{CuInS}_2/\text{ZnS}$ quantum dots was also shown. Difference of 71 meV between the CuInS_2 cores and $\text{CuInS}_2/\text{ZnS}$ QD's emission energy was noticed. Temporal evolution of the PL maxima were shown in the figure (b) and (d). Obtained results give a strong premise that PL maximum shifts (b) and (d) are not related to the surface of the QDs. Possible explanation of the results assume competitive recombination from the states characterized by different decay rates.

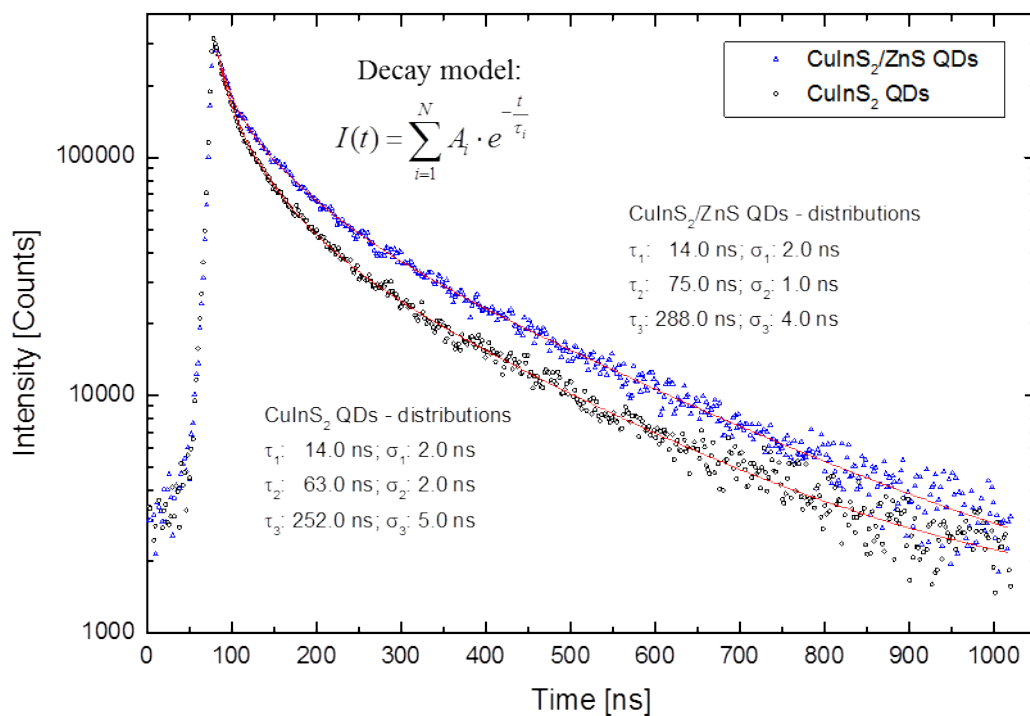


Fig. 9s Luminescence decay curves measured for the *ca.* 3.0 nm core CuInS₂ (black dots) as well as for their corresponding (b) CuInS₂/ZnS core-shell quantum heterostructures (blue triangles). Samples were excited by <100 fs pulses with λ_{ex} = 550 nm.

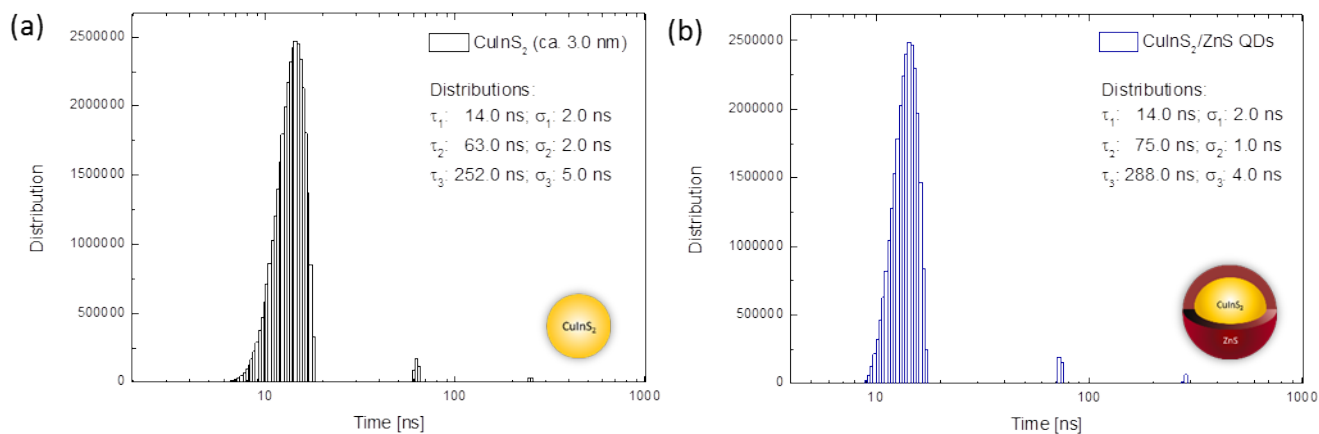


Fig. 10s Luminescent lifetime distributions calculated for the *ca.* 3.0 nm core CuInS₂ as well as for their corresponding (b) CuInS₂/ZnS core-shell quantum heterostructures. Three different distributions, characterized by significantly different decay rates are noticed for all the quantum dots.